Supporting Information

Strategies for Enhancing the Rate Constant of C–H Bond Cleavage by Concerted Proton-Coupled Electron Transfer

Elvira R. Sayfutyarova, Yan Choi Lam, and Sharon Hammes-Schiffer*

Department of Chemistry, Yale University, 225 Prospect Street, New Haven, Connecticut 06520

*Corresponding author email: sharon.hammes-schiffer@yale.edu

Table of Contents

Optimized structures for the studied species

We optimized the geometries of the reactant and product using unrestricted density functional theory (DFT) with the B3LYP[1-2] functional and the 6-31+G**[3-5] basis set with the Gaussian 09 program.[6] The structures were optimized in solution (acetonitrile) using the conductor-like polarizable continuum model (CPCM).[7] Table S1 contains the optimized equilibrium proton donor-acceptor C–O distances for the reactant and product states of each molecule. Tables S13-S20 provide the optimized Cartesian coordinates for both the reactant and product structures for the fluorenyl-benzoates studied.

Table S1. Equilibrium and Average Proton Donor-Acceptor Distances from Optimized Reactant and Product States (in Å)

Substituent X	Reactant	Product	Average
NH_2	2.957	2.928	2.942
OMe	2.968	2.943	2.955
H	3.029	2.972	3.000
CF_3	3.069	2.993	3.031

Reactant and product structures for a range of proton donor-acceptor distances

The total rate constant k_{PCET} is obtained by calculating the rate constants $k(R)$ for a range of proton donor-acceptor distances R and integrating over R, weighting each value by the probability distribution function $P(R)$. The calculation of the rate constant $k(R)$ at a given proton donor-acceptor distance R requires geometries for both the reactant and product states with the same R. Thus, for each molecule we first optimized both the reactant and product structures while constraining the proton donor-acceptor distance R to the average equilibrium distance R_{av}, as obtained by averaging the equilibrium proton donor-acceptor distances R for the reactant and product structures (Table S1). Then for each molecule we performed a series of such constrained geometry optimizations for the reactant and product states for a range of R, varying its value with a 0.05 Å increment/decrement starting from this average distance R_{av}.

We generated reactant and product structures for R ranging from 2.400 Å to 3.400 Å for (o-Flr)(p-H)$C_6H_3COO^-$, 2.431 Å to 3.431 Å for (o-Flr)(p-CF_3)$C_6H_3COO^-$, 2.355 Å to 3.355 Å for (o-Flr)(p-OMe)$C_6H_3COO^-$, and 2.342 Å to 3.342 Å for (o-Flr)(p-NH_2)$C_6H_3COO^-$ (i.e., spanning the range from –0.6 Å to 0.4 Å from R_{av} for each molecule). The computed electronic energies for the reactant and product states for all molecules are depicted in Figure S1.

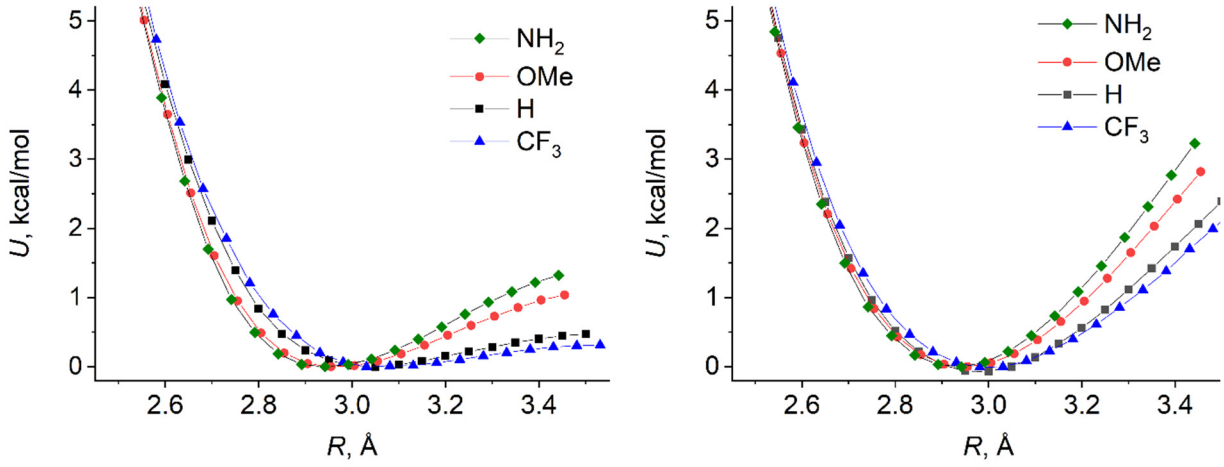

Figure S1. Electronic energies of geometries obtained from constrained geometry optimizations with the proton donor-acceptor distance R constrained for the reactant (left) and product (right) states. The calculations were performed with DFT/B3LYP/6-31++G** in acetonitrile.

Average structures

The calculation of the proton potentials at a given R should be performed for a structure corresponding to the crossing point between the reactant and product states of a given molecule along an inner-sphere solute coordinate. We model this structure as an intermediate structure between the reactant and product structures. Because the reactant and the product have significantly different geometries due to the change of hybridization of the donor carbon atom from sp^3 to sp^2, we used internal coordinates to average the reactant and product structures for each R. The algorithm to generate an average structure for a given proton donor-acceptor distance R can be described as follows. The positions of the donor and acceptor atoms were fixed at (0,0,0) and (0,0,R), respectively, for both the reactant and product structures, ensuring that the donor carbon and acceptor oxygen are in identical positions for both structures. The positions of the other atoms were defined using the averaged internal coordinates corresponding to bond lengths, angles, and dihedrals obtained for the optimized reactant and product structures at each R.

Proton potentials

For each average structure at a given proton donor-acceptor distance *R*, we performed additional constrained geometry optimizations with all atoms except the transferring proton fixed to find the optimized position of the hydrogen on the donor (for the reactant state) and on the acceptor (for the product state). The one-dimensional proton coordinate axis was defined to be the line connecting these two optimized positions of the proton at a given proton donor-acceptor distance *R*. Then single-point DFT energy calculations were performed along this axis to obtain the proton potentials. Proton potentials were generated for *R* ranging from 2.400 Å to 3.400 Å for (o-Flr)(p-H)$C_6H_3COO^-$, 2.431 Å to 3.431 Å for (o-Flr)(p-CF_3)$C_6H_3COO^-$, 2.355 Å to 3.355 Å for (o-Flr)(p-OMe)$C_6H_3COO^-$, and 2.342 Å to 3.342 Å for (o-Flr)(p-NH_2)$C_6H_3COO^-$. Figures S2 and S3 depict ten pairs of proton potentials for *R* ranging from the average equilibrium distance R_{av} to R_{av} –0.5 Å for each molecule, where the distances shorter than or equal to the equilibrium distance tend to contribute the most to the rate constants.

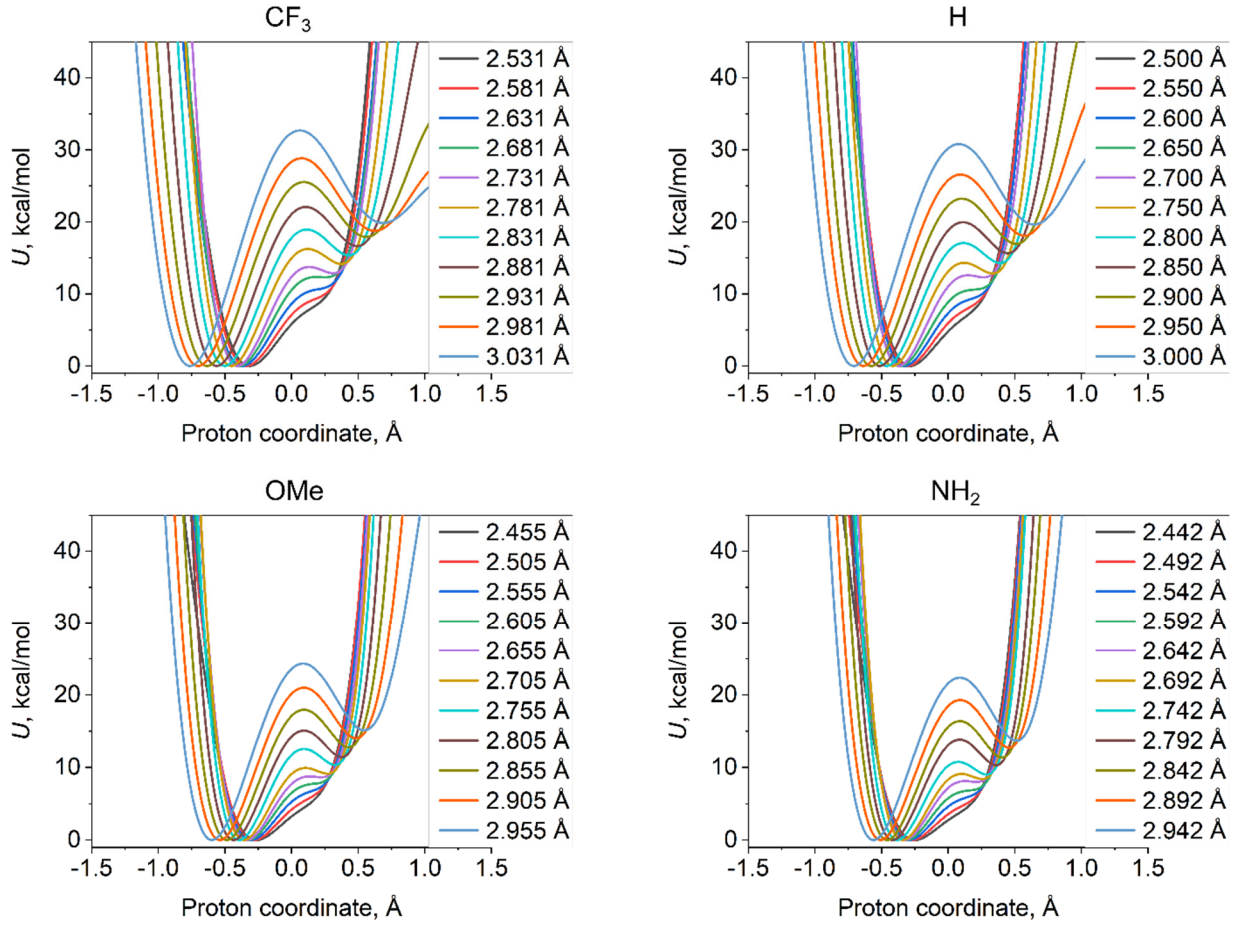

Figure S2. Proton potentials for the reactant structures for the range of proton donor-acceptor distances specified.

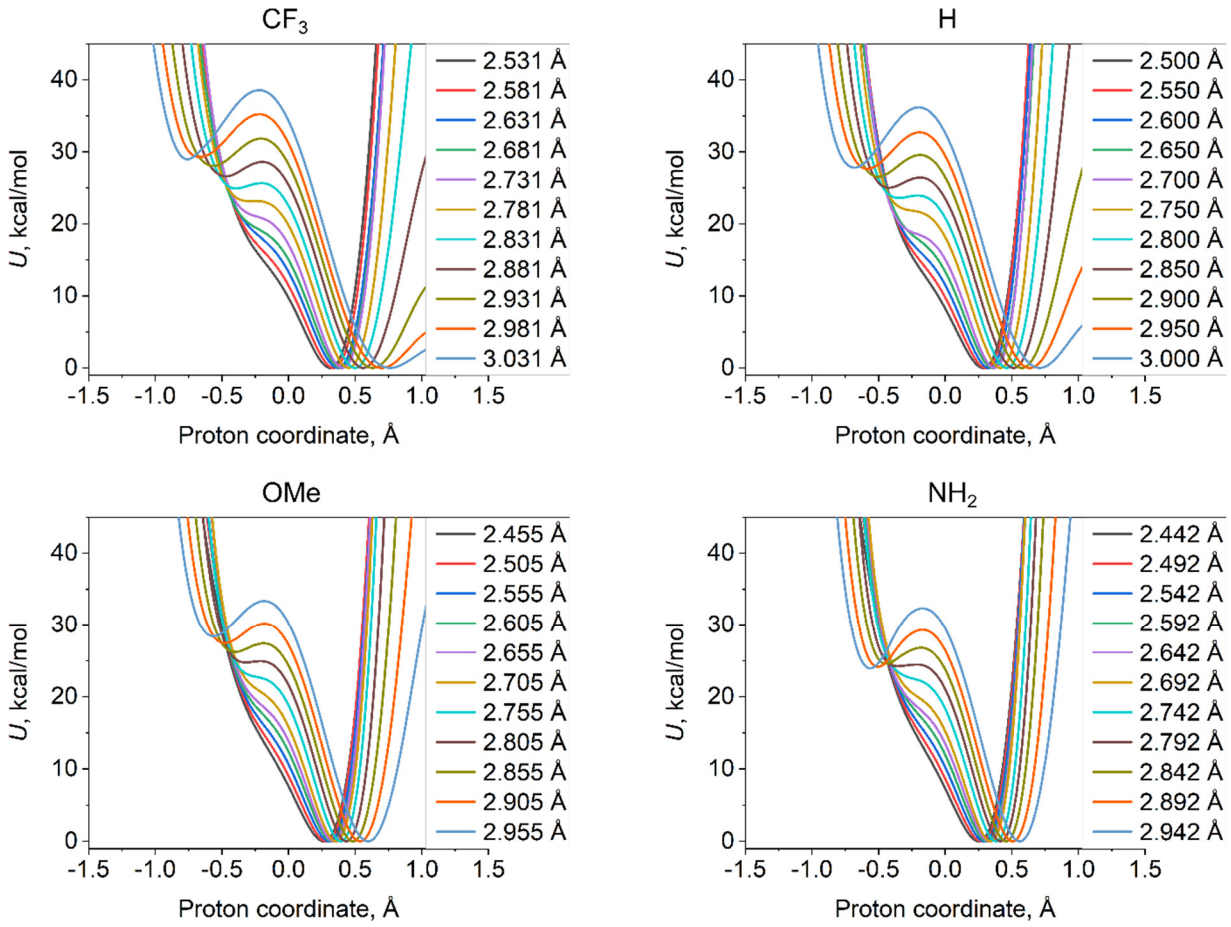

Figure S3. Proton potentials for the product structures for the range of proton donor-acceptor distances specified.

Probability distribution function for proton donor-acceptor distance

The probability distribution function $P(R)$ is an exponential function of the potential energy U of the reactant at proton donor-acceptor distance R relative to the potential energy U at the equilibrium distance R_0. Setting $U(R_0) = 0$, this function can be expressed as:

$$P(R) = C_N \exp\left[-\frac{U(R)}{k_B T}\right] = C_N \exp\left[-\beta U(R)\right] \quad \text{(S1)}$$

where $\beta = 1/k_B T$. This probability distribution function was calculated directly from the electronic energies $U(R)$ obtained from the constrained geometry optimizations of the reactant (Figure S1, left side). Due to the shape of the energy profile $U(R)$, it is not possible to normalize $P(R)$. The normalization constant C_N is not relevant when computing only relative rate constants for different oxidants, but it could vary for different substituents on the fluorenyl-benzoate molecules. For simplicity, this normalization constant is assumed to be approximately the same for all species studied in this work. The agreement between the calculated Brønsted α (slope) and the experimentally measured value for the series of different substituents suggests that this assumption is reasonable.

Total reorganization energy

A. Inner sphere (solute) reorganization energy

To compute the inner-sphere reorganization energy associated with each molecule, we used the four-point method:

$$\lambda_{i,\mathrm{mol}} = \frac{1}{2}\left(\lambda_1 + \lambda_2\right), \quad \text{(S2)}$$

with

$$\lambda_1 = E_{\mathrm{reactant}}\left(g_{\mathrm{product}}\right) - E_{\mathrm{reactant}}\left(g_{\mathrm{reactant}}\right) \quad \text{(S3)}$$

$$\lambda_2 = E_{\mathrm{product}}\left(g_{\mathrm{reactant}}\right) - E_{\mathrm{product}}\left(g_{\mathrm{product}}\right) \quad \text{(S4)}$$

where $E_A(g_B)$ denotes the energy of state A at the optimized geometry of state B. Only the electronic energies are required for the calculation of inner-sphere reorganization energies. These electronic energies were computed in the gas phase using the geometries optimized with CPCM. For PCET reactions, both the electron and the proton are on their donors for the reactant or on their acceptors for the product. Thus, the calculation of the energy $E_A(g_B)$ when the geometry B does not correspond to the optimized geometry for state A requires the optimization of the proton on the donor or acceptor with all other nuclei fixed. The inner sphere reorganization energies obtained using the computed energies in Table S2 are given in Table S3.

Table S2. Electronic Energies in Gas Phase at Geometries Optimized in Acetonitrile for Computing the Inner-Sphere Reorganization Energies of the Fluorenyl-Benzoates

Species	**Geometry**	**Electronic energy, a.u.**			
		X=NH_2	X=OMe	X=H	X=CF_3
Reactant	Reactant	-975.917433	-1035.085862	-920.557127	-1257.625233
Reactant	Product	-975.872408	-1035.040456	-920.511347	-1257.576788
Product	Product	-975.830562	-1034.995464	-920.464923	-1257.521060
Product	Reactant	-975.788168	-1034.952777	-920.420236	-1257.475258

Table S3. Inner-Sphere Reorganization Energies (in kcal/mol)

Molecule	$\lambda_{i,\mathrm{mol}}$
(o-Flr)(p-NH_2)$C_6H_3COO^-$	27.4
(o-Flr)(p-OMe)$C_6H_3COO^-$	27.6
(o-Flr)(p-H)$C_6H_3COO^-$	28.4
(o-Flr)(p-CF_3)$C_6H_3COO^-$	29.6
$FeCp_2^+$	0.18
$NAr_3^{\bullet+}$	2.58

We also calculated the inner-sphere reorganization energy associated with the oxidants with the same four-point method. In this case, we calculated the electronic energies for both the oxidized and reduced species of the two oxidants in the gas phase at the corresponding geometries optimized in solution phase (Table S4). The resulting inner-sphere reorganization energies are given in Table S3.

Table S4. Electronic Energies in Gas Phase at Geometries Optimized in Acetonitrile for Computing the Inner-Sphere Reorganization Energy of the Oxidants (in a.u.)

Species	Geometry	$FeCp_2^+$	$N(Ar_{OMe})_3^{\bullet+}$
Oxidized	Oxidized	-1650.487645	-1091.915517
Oxidized	Reduced	-1650.747371	-1092.143521
Reduced	Reduced	-1650.747772	-1092.147575
Reduced	Oxidized	-1650.487463	-1091.911346

B. Outer sphere (solvent) reorganization energy

To evaluate the outer sphere (solvent) reorganization energy, we used the two-sphere model because it is difficult to determine how the oxidant molecule approaches the fluorenyl-benzoate molecule in terms of location, distance, and orientation. The equation used for the two-sphere model, assuming the two spheres are touching, is:

$$\lambda_S = (\Delta q)^2 \left(\frac{1}{\varepsilon_{\text{opt}}} - \frac{1}{\varepsilon_{\text{static}}} \right) \left(\frac{1}{2R_A} + \frac{1}{2R_B} - \frac{1}{R_A + R_A} \right). \quad \text{(S5)}$$

For acetonitrile, the static dielectric constant $\varepsilon_{\text{static}}$ is 35.688, and the optical dielectric constant ε_{opt} is 1.806874. The radii of the spheres were determined from the cavity volumes from CPCM calculations at the optimized structures, assuming a sphere with volume equal to the cavity volume (Table S5). The resulting calculated solvent reorganization energies λ_S and total reorganization energies λ are presented in Table S6. The total reorganization energy is ~50 kcal/mol for all systems studied.

Table S5. Cavity Volumes and Radii of Spheres for Molecules Studied

Species	Cavity volume, Å^3	Radius, Å
(o-Flr)(p-NH_2)$C_6H_3COO^-$	407.382	4.599
(o-Flr)(p-OMe)$C_6H_3COO^-$	416.519	4.633
(o-Flr)(p-H)$C_6H_3COO^-$	386.748	4.520
(o-Flr)(p-CF_3)$C_6H_3COO^-$	417.309	4.636
$FeCp_2^+$	224.200	3.769
$N(Ar_{OMe})_3^{\bullet+}$	456.126	4.775

Table S6. Total Reorganization Energy and Components (in kcal/mol)

Molecule	Oxidant	$\lambda_{i,\mathrm{mol}}$	$\lambda_{i,\mathrm{ox}}$	λ_S	λ
(o-Flr)(p- NH_2)$C_6H_3COO^-$	$FeCp_2^+$	27.4	0.18	21.3	48.88
	$N(Ar_{OMe})_3^{\bullet+}$	27.4	2.58	18.6	48.58
(o-Flr)(p-OMe)$C_6H_3COO^-$	$FeCp_2^+$	27.6	0.18	21.2	48.98
	$N(Ar_{OMe})_3^{\bullet+}$	27.6	2.58	18.6	48.78
(o-Flr)(p-H)$C_6H_3COO^-$	$FeCp_2^+$	28.4	0.18	21.4	49.98
	$N(Ar_{OMe})_3^{\bullet+}$	28.4	2.58	18.8	49.78
(o-Flr)(p-CF_3)$C_6H_3COO^-$	$FeCp_2^+$	29.6	0.18	21.2	50.98
	$N(Ar_{OMe})_3^{\bullet+}$	29.6	2.58	18.6	50.78

Change in the free energy due to the substituents

Table S7 presents the Gibbs free energies for the reactant and product structures in acetonitrile. Using the values in Table S7, we computed the $\Delta\Delta G^0$ with respect to the (o-Flr)(p-CF_3)$C_6H_3COO^-$ species (Table S8) to assess the change in reaction free energy ΔG^0 with the change in basicity due to the substituted functional group as:

$$\Delta\Delta G^0 = [G^0_{\mathrm{product}}(\mathrm{X}) - G^0_{\mathrm{reactant}}(\mathrm{X})] - [G^0_{\mathrm{product}}(\mathrm{CF_3}) - G^0_{\mathrm{reactant}}(\mathrm{CF_3})] \quad \text{(S6)}$$

Table S7. Gibbs Free Energies in Acetonitrile at Geometries Optimized in Acetonitrile

Species	Gibbs Free Energy, a.u.			
	X=NH_2	X=OMe	X=H	X=CF_3
Reactant	-975.774912	-1034.925481	-920.423656	-1257.488767
Product	-975.610978	-1034.758852	-920.254392	-1257.313078

Table S8. ΔG^0 and $\Delta\Delta G^0$ for Substituted Fluorenyl-Benzoates Reacting with $FeCp_2^+$

Substituent X	$\Delta\Delta G^0$, kcal/mol	ΔG^0, kcal/mol
NH_2	-7.38	-14.35
OMe	-5.69	-12.66
H	-4.03	-11.0
CF_3	0.00	-6.97

Dominant proton donor-acceptor distance

The rate constant at a given proton donor-acceptor distance R can be written as:

$$k(R) = \frac{1}{\hbar}\sqrt{\frac{\pi}{k_B T \lambda}} \sum_{\mu,\nu} P_\mu \left| S_{\mu\nu}(R) V^{\mathrm{el}} \right|^2 \exp\left(-\frac{\Delta G^{\ddagger}_{\mu\nu}}{k_B T} \right), \tag{S7}$$

where $\Delta G^{\ddagger}_{\mu\nu} = \frac{\left(\Delta G^0_{\mu\nu} + \lambda\right)^2}{4\lambda}$, and the various quantities are defined in the main paper. The total rate constant k_{PCET} is given by:

$$k_{\mathrm{PCET}} = \int_0^\infty k(R) P(R) dR \,. \tag{S8}$$

Note that $\Delta G^0_{\mu\nu} = \Delta G^0 + \epsilon_\nu - \epsilon_\mu$, where ϵ_μ and ϵ_ν are the energies of the reactant vibronic state μ and the product vibronic state ν relative to their respective ground vibronic states (i.e., $\Delta G^0_{00} = \Delta G^0$).

The electronic coupling corresponding to outer-sphere electron transfer from the fluorenyl-benzoates to the external oxidant is not known, but it is assumed to be independent of the proton donor-acceptor distance R and to be the same for all molecules and all oxidants in this study. In this case, it does not impact the Brønsted α (slope) and simply shifts the curve along the $\log k_{\mathrm{PCET}}$ axis.

To analyze the results, we identify the dominant proton donor-acceptor distance, which is defined as the distance R with the greatest value of the integrand in the thermal averaging used to produce the total rate constant k_{PCET}. Thus, the dominant proton donor-acceptor distance is the maximum of $k(R)P(R)$ (Figures S4, S5). To estimate the maximum of $k(R)P(R)$, we fitted $k(R)P(R)$ to Gaussian distribution.

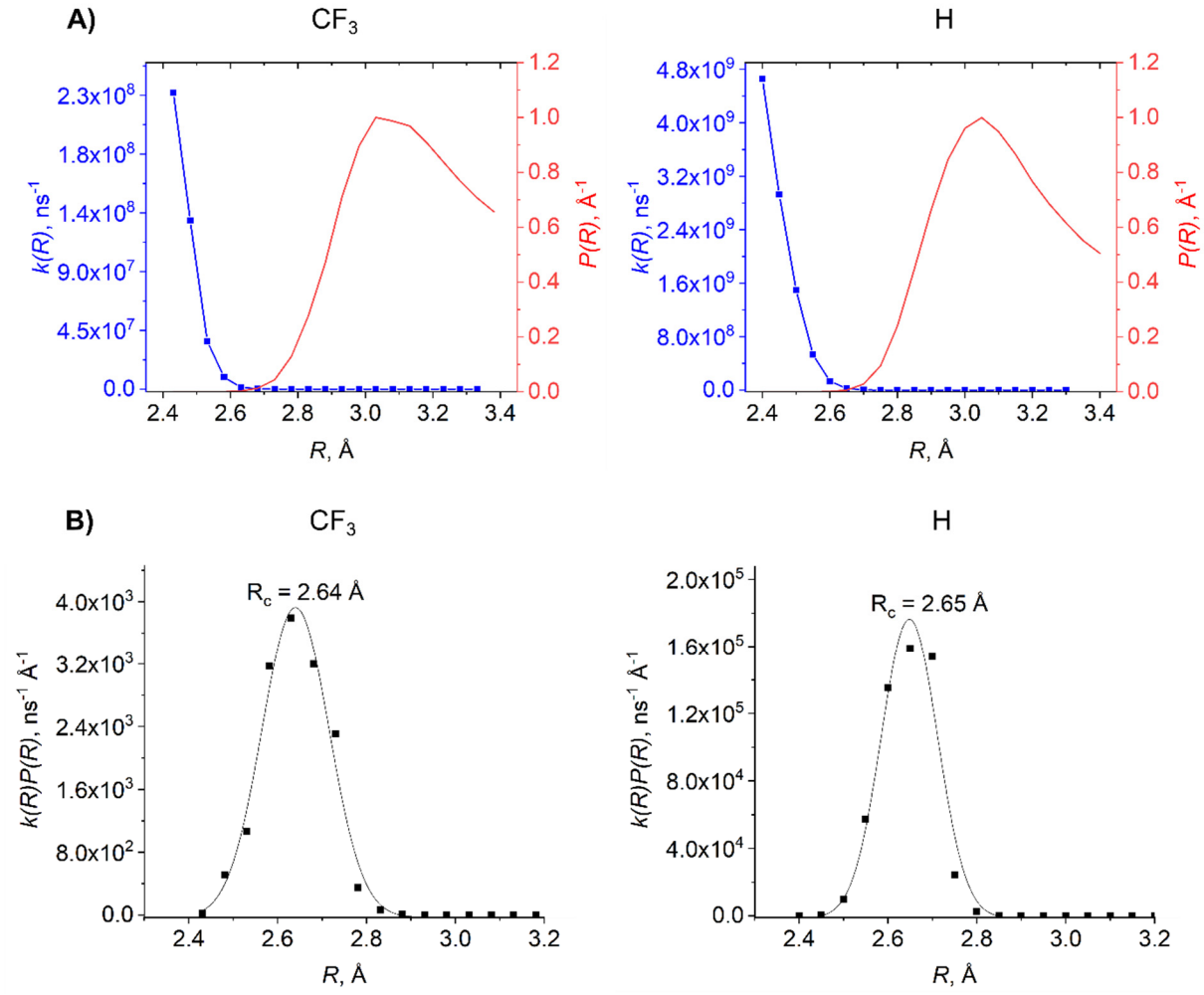

Figure S4. Probability distribution function $P(R)$ and rate constant $k(R)$ (A), and the product $k(R)P(R)$ of these two quantities (B), computed at $\Delta G^0 = -11.0$ kcal/mol for (o-Flr)(p-H)$C_6H_3COO^-$ and at $\Delta G^0 = -6.97$ kcal/mol for (o-Flr)(p-CF_3)$C_6H_3COO^-$, i.e., at the estimated ΔG^0 for the oxidant $FeCp_2^+$. Note that the magnitudes of the rate constants depend on constants that are not well-defined, so only the relative rate constants are meaningful.

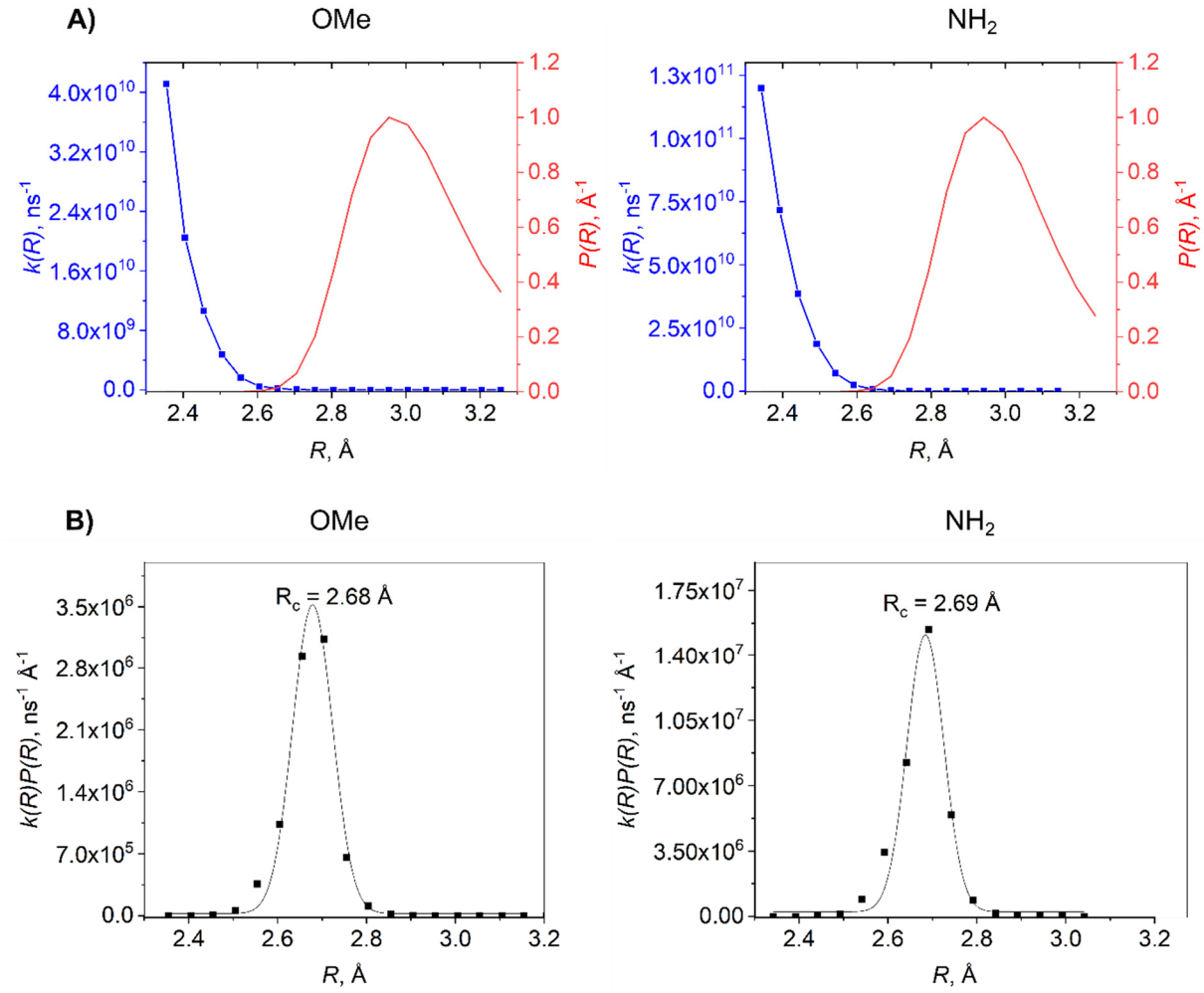

Figure S5. Probability distribution function $P(R)$ and rate constant $k(R)$ (A), and the product $k(R)P(R)$ of these two quantities (B), computed at $\Delta G^0 = -12.66$ kcal/mol for (o-Flr)(p-OMe)$C_6H_3COO^-$ and at $\Delta G^0 = -14.35$ kcal/mol for (o-Flr)(p-NH_2)$C_6H_3COO^-$, i.e., at the estimated ΔG^0 for the oxidant $FeCp_2^+$. Note that the magnitudes of the rate constants depend on constants that are not well-defined, so only the relative rate constants are meaningful.

Table S9. Dominant distances *R evaluated for different oxidants with λ=30 kcal/mol[a]**

Molecule	$FeCp^*Cp^+$	$FeCp_2^+$	$N(Ar_{OMe})_3^{\bullet+}$	$N(Ar_{OMe})_2(Ar_{Br})^{\bullet+}$
(o-Flr)(p-NH_2)$C_6H_3COO^-$	2.70	2.69	2.68	2.69
(o-Flr)(p-OMe)$C_6H_3COO^-$	2.70	2.68	2.68	2.68
(o-Flr)(p-H)$C_6H_3COO^-$	2.67	2.65	2.66	2.68
(o-Flr)(p-CF_3)$C_6H_3COO^-$	2.67	2.64	2.64	2.65

[a] The grid along the proton donor-acceptor coordinate R was 0.05 Å, and the dominant distance R^* was determined as the peak of a Gaussian fit of $k(R)P(R)$. The value of R^* is the same for all oxidants for each molecule to within the numerical precision provided by this methodology.

Calculated rate constants

Table S10 provides the rate constants computed with electronic coupling V^{el} = 1 kcal/mol. We did not normalize $P(R)$ due to the shape of the reactant energy profile $U(R)$ (Figure S1). The values of V^{el} and the normalization constant C_N for $P(R)$ are assumed to be the same for all systems studied in this work and therefore do not impact the slope but rather just shift the curve along the $\log k_{PCET}$ axis. Thus, this table provides only estimates of relative rate constants.

Table S10. Relative Rate Constants Computed for Different Total Reorganization Energies and Driving Forces with λ=30 kcal/mol.[a]

ΔG^0, kcal/mol	k_{PCET}			
	X=NH_2	X=OMe	X=H	X=CF_3
-1.0	2.582×10^{4}	1.105×10^{4}	8.843×10^{2}	3.065×10^{2}
-4.0	1.603×10^{5}	6.803×10^{4}	6.738×10^{3}	2.162×10^{3}
-7.0	8.579×10^{5}	3.685×10^{5}	4.696×10^{4}	1.442×10^{4}
-9.0	2.441×10^{6}	1.069×10^{6}	1.626×10^{5}	4.943×10^{4}
-11.0	6.601×10^{6}	2.971×10^{6}	5.431×10^{5}	1.654×10^{5}
-13.0	1.710×10^{7}	7.967×10^{6}	1.769×10^{6}	5.468×10^{5}
-15.0	4.303×10^{7}	2.082×10^{7}	5.710×10^{6}	1.812×10^{6}
-18.0	1.716×10^{8}	8.681×10^{7}	3.352×10^{7}	1.134×10^{7}
-20.0	4.562×10^{8}	2.292×10^{8}	1.106×10^{8}	3.960×10^{7}
-23.0	2.345×10^{9}	1.049×10^{9}	6.608×10^{8}	2.611×10^{8}
-25.0	7.783×10^{9}	3.012×10^{9}	2.127×10^{9}	8.992×10^{8}
-27.0	2.679×10^{10}	8.806×10^{9}	6.617×10^{9}	2.984×10^{9}

[a] Note that the magnitudes of the rate constants are not meaningful because they assume arbitrary values of the electronic coupling and normalization constant.

Linear Relationship between ΔG^0 and the Hammett Constant σ

Figure S6 shows the linear relationship between the PCET reaction free energy, ΔG^0, and the Hammett parameter σ characterizing the electronic properties of the para-substituent.[8] Given the hydrogen bond between the weakly acidic fluorenyl C—H and the benzoate, the equilibrium proton donor-acceptor distance R_0 is a function of the Hammett parameter σ: more electron-donating substituents (i.e., more negative σ) lead to shorter equilibrium distances, as shown in Table 1 in the main text. The potential energy at any distance R relative to the energy at R_0, $U(R)$, can also be treated as a function of σ. The rate constant $k(R)$ at fixed proton donor-acceptor distance R is a function of the reaction free energy ΔG^0, and the probability distribution function $P(R)$ is a function of $U(R)$. Hence, the total rate constant k calculated in Eq. (3) or Eq. (7) in the main text is a function of σ and the redox potential of the oxidant, E_{ox}.

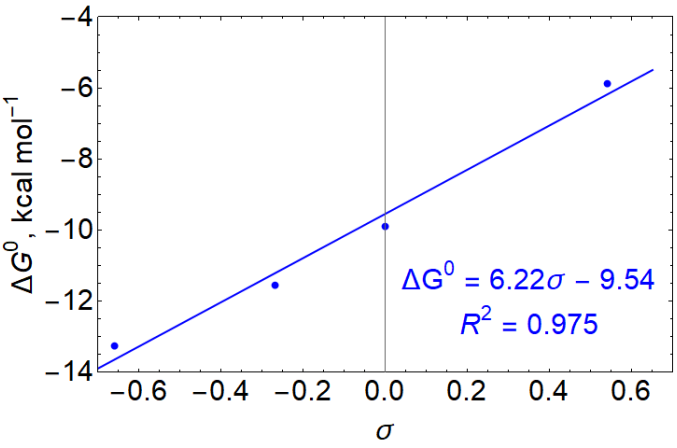

Figure S6. Reaction free energy, ΔG^0, for the oxidative PCET of fluorenyl-benzoates with $FeCp_2^+$ as the oxidant, as a function of the Hammett constant of the para-substituent on the benzoate.

Calculated Brønsted α

As shown in Eq. (11) in the main paper, the Brønsted α for changing the oxidant with a given para-substituent (fixed σ) can be evaluated from the following expression:

$$\left.\frac{\partial \log k_{\mathrm{PCET}}}{\partial \log K_{\mathrm{eq}}}\right|_{\sigma} = \left.\frac{\partial \log k(R^*)}{\partial \log K_{\mathrm{eq}}}\right|_{\sigma} = \frac{1}{2} + \sum_{\mu,\nu} \omega_{\mu,\nu} \frac{\Delta G^0_{\mu,\nu}}{2\lambda} = \frac{1}{2} + \frac{\Delta G^0}{2\lambda} + \sum_{\mu,\nu} \omega_{\mu,\nu} \frac{\Delta \epsilon_{\mu,\nu}}{2\lambda} \tag{S9}$$

The Brønsted α computed with total reorganization energy λ = 30 kcal/mol and the oxidant $FeCp_2^+$, as well as the individual components given in Eq. (S9), are presented in Table S11. Table S12 provides the Brønsted α for changing substituents computed using the approximate form given in Eq. (12) and using the full PCET rate constant given in Eq. (3), as well as experimental values, for different oxidants.

Table S11. Brønsted α and Components for the $FeCp_2^+$ Oxidant with λ=30 kcal/mol

Substituent X	ΔG^0, kcal/mol[a]	$\frac{1}{2} + \frac{\Delta G^0}{2\lambda}$	$\sum_{\mu,\nu} \omega_{\mu,\nu} \frac{\Delta \epsilon_{\mu,\nu}}{2\lambda}$ [b]	$\left.\frac{\partial \log k(R^*)}{\partial \Delta G^0}\right\|_{E_{\mathrm{ox}},\sigma}$ [c]
NH_2	-14.35	0.261	0.012	0.273
OMe	-12.66	0.289	0.010	0.299
H	-11.0	0.317	0.031	0.348
CF_3	-6.97	0.384	-0.011	0.373

[a] These free energies are estimated for $FeCp_2^+$, as given in Table S8.
[b] These values were evaluated at the grid point corresponding to the value of *R* closest to the dominant value *R**, where the grid spacing along the proton donor-acceptor coordinate *R* was 0.05 Å.
[c] This column is the sum of the previous two columns, as given in Eq. (S9), and is the same as the values given in Table 1 of the main paper.

Table S12. Brønsted α computed for different oxidants with λ=30 kcal/mol

Method	$FeCp^*Cp^+$	$FeCp_2^+$	$N(Ar_{OMe})_3^{\bullet+}$	$N(Ar_{OMe})_2(Ar_{Br})^{\bullet+}$
Full calculations [a]	0.71	0.63	0.58	0.54
Results using Eq. 12[b]	0.48–0.52	0.46–0.53	0.47–0.51	0.47–0.51
Experiment [c]	0.61 ± 0.09	0.58 ± 0.10	0.48 ± 0.05	0.36 ± 0.07

[a] These values correspond to the slope of a linear fit to a Brønsted plot composed of the PCET rate constants obtained from the full PCET rate constant given in Eq. (3).
[b] The ranges correspond to the approximate expression in Eq. (12) for the four substituents listed in Table 1 of the main paper.

[c] Experimental data from Ref.[9]

Cartesian coordinates of optimized equilibrium structures

Table S13. Reactant Structure for X= H (-920.64802497 E_h)

atom	x	y	z
C	19.864323	-29.134424	10.478145
C	19.063292	-28.178535	11.119552
C	19.393209	-26.817167	11.061904
C	20.528171	-26.425379	10.355798
C	21.332336	-27.386735	9.706260
C	21.005100	-28.746017	9.767295
H	19.595838	-30.185585	10.532790
H	18.179730	-28.495883	11.665984
H	18.767389	-26.081227	11.559854
H	21.621014	-29.491705	9.272092
C	22.444986	-26.691738	9.042268
C	22.316972	-25.307298	9.285846
C	23.245349	-24.410756	8.761706
C	24.307712	-24.903534	7.991030
C	24.437277	-26.279409	7.751818
C	23.507679	-27.183977	8.276099
H	23.148570	-23.343576	8.942187
H	25.036998	-24.214058	7.575404
H	25.266263	-26.645719	7.152961
H	23.613639	-28.248600	8.086519
C	20.125757	-23.992020	9.634516
C	19.615419	-24.159463	8.335221
C	18.694891	-23.266003	7.789575
C	18.248230	-22.183716	8.556577
C	18.724029	-22.023048	9.856840
C	19.670613	-22.905044	10.411220
H	19.951538	-25.006810	7.742639
H	18.326934	-23.414170	6.778170
C	20.152473	-22.613888	11.836724
C	21.110667	-25.027618	10.173072
O	21.398914	-22.671735	12.054307
O	19.260184	-22.311027	12.679483
H	17.53128	-21.47765	8.146691
H	18.36578	-21.20058	10.46831
H	21.47444	-24.65521	11.13772

Table S14. Product Structure for X= H (-920.47896892 E_h)

atom	x	y	z
C	20.017349	-29.059994	11.030332
C	18.994545	-28.110613	11.177418
C	19.143503	-26.815112	10.672633
C	20.339490	-26.473199	10.020904
C	21.371804	-27.449674	9.859128
C	21.211186	-28.735369	10.363766
H	19.882010	-30.060854	11.428977
H	18.075559	-28.385684	11.685881
H	18.339016	-26.093730	10.780193
H	21.988211	-29.484947	10.243896
C	22.462980	-26.822097	9.104802
C	22.067660	-25.478420	8.809916
C	22.936966	-24.626694	8.106625
C	24.176126	-25.121276	7.689052
C	24.554344	-26.442833	7.972997
C	23.699598	-27.300328	8.687093
H	22.657519	-23.599801	7.892073
H	24.855143	-24.474644	7.141718
H	25.522040	-26.806981	7.641357
H	24.009742	-28.318006	8.906434
C	19.965554	-24.012120	9.243552
C	19.713529	-23.525233	7.944768
C	18.894662	-22.418565	7.727424
C	18.295969	-21.766841	8.809739
C	18.540277	-22.221074	10.103841
C	19.381485	-23.320364	10.338166
H	20.139671	-24.052764	7.097802
H	18.715012	-22.074803	6.713420
C	19.655808	-23.625343	11.780720
C	20.760656	-25.242189	9.383345
O	20.879987	-24.088225	12.119018
O	18.846210	-23.420846	12.668354
H	17.652299	-20.908214	8.648443
H	18.101732	-21.712747	10.955515
H	21.449477	-24.206237	11.339827

Table S15. Reactant Structure for X= CF_3 (-1257.70956393 E_h)

atom	x	y	z
C	19.876413	-29.141771	10.486446
C	19.084276	-28.192525	11.148148
C	19.418958	-26.831737	11.107655
C	20.549872	-26.435430	10.398030
C	21.345183	-27.389399	9.727746
C	21.012949	-28.747955	9.771856
H	19.604236	-30.192524	10.528118
H	18.203988	-28.514328	11.697082
H	18.800390	-26.100977	11.621896
H	21.621737	-29.488789	9.261003
C	22.455231	-26.689233	9.064555
C	22.335944	-25.308083	9.328637
C	23.262646	-24.406916	8.810052
C	24.316337	-24.893031	8.023432
C	24.438065	-26.265774	7.763819
C	23.509398	-27.174430	8.282593
H	23.172256	-23.342219	9.007239
H	25.044928	-24.200647	7.611660
H	25.260595	-26.626720	7.153014
H	23.609591	-28.236531	8.076946
C	20.151552	-23.995788	9.706046
C	19.630074	-24.156786	8.412370
C	18.709585	-23.251254	7.888426
C	18.275291	-22.164897	8.661574
C	18.767365	-22.016677	9.952315
C	19.713521	-22.909758	10.489404
H	19.952692	-25.001334	7.812571
C	18.187784	-23.406264	6.490737
C	20.215175	-22.636335	11.911660
C	21.136929	-25.036990	10.229523
O	21.467533	-22.614160	12.083434
O	19.325862	-22.432648	12.783994
H	17.557832	-21.454171	8.263835
H	18.418811	-21.194790	10.569102
H	21.507045	-24.676805	11.195942
F	18.529353	-24.587306	5.918325
F	18.648722	-22.427849	5.653511
F	16.827279	-23.324919	6.432262

Table S16. Product Structure for X= CF_3 (-1257.53543967 E_h)

atom	x	y	z
C	20.038639	-29.091649	11.064327
C	19.016873	-28.143491	11.223264
C	19.161246	-26.846133	10.721871
C	20.352417	-26.501631	10.062696
C	21.383259	-27.477314	9.887769
C	21.226996	-28.764540	10.388760
H	19.906905	-30.093983	11.460327
H	18.101993	-28.420621	11.737789
H	18.356113	-26.126856	10.837798
H	22.002776	-29.513695	10.259291
C	22.467992	-26.847381	9.125773
C	22.071292	-25.502565	8.839015
C	22.935142	-24.647923	8.132706
C	24.170116	-25.141925	7.702061
C	24.549163	-26.464806	7.976941
C	23.700142	-27.324756	8.695318
H	22.657200	-23.619030	7.925890
H	24.844892	-24.493335	7.151988
H	25.513456	-26.828511	7.635220
H	24.011536	-28.343403	8.907852
C	19.976235	-24.038117	9.302267
C	19.726118	-23.534910	8.009573
C	18.915724	-22.419953	7.817250
C	18.319408	-21.774954	8.907924
C	18.564181	-22.251193	10.190056
C	19.400257	-23.357908	10.404325
H	20.147943	-24.050467	7.155445
C	18.641429	-21.902134	6.429149
C	19.671113	-23.692303	11.844832
C	20.769500	-25.270031	9.424997
O	20.907078	-24.114479	12.182913
O	18.839859	-23.542456	12.720843
H	17.682343	-20.909566	8.761389
H	18.126673	-21.752594	11.047351
H	21.493630	-24.185813	11.410981
F	19.351394	-22.545494	5.473873
F	18.936485	-20.578899	6.317004
F	17.327590	-22.026592	6.093170

Table S17. Reactant Structure for X= OMe (-1035.17909873 E_h)

atom	x	y	z
C	19.850376	-29.124173	10.450546
C	19.057876	-28.176804	11.115021
C	19.398310	-26.817135	11.087796
C	20.534813	-26.417831	10.388137
C	21.330182	-27.370617	9.715148
C	20.992789	-28.728490	9.746407
H	19.573852	-30.174212	10.481922
H	18.172776	-28.499706	11.655717
H	18.779232	-26.087734	11.603554
H	21.602137	-29.467450	9.233251
C	22.446226	-26.669039	9.064089
C	22.328546	-25.289324	9.339042
C	23.262155	-24.387993	8.832315
C	24.319069	-24.870990	8.048141
C	24.438560	-26.242183	7.778264
C	23.503797	-27.151574	8.284667
H	23.173535	-23.324392	9.036740
H	25.052215	-24.177562	7.646033
H	25.263725	-26.600879	7.169588
H	23.601947	-28.212528	8.071617
C	20.152288	-23.960244	9.737670
C	19.618834	-24.125620	8.444401
C	18.697388	-23.216683	7.922695
C	18.278176	-22.130555	8.708143
C	18.785032	-21.984861	9.991404
C	19.736100	-22.874654	10.533161
H	19.940761	-24.978548	7.857876
O	18.147745	-23.300994	6.670940
C	20.243436	-22.580429	11.948585
C	21.129391	-25.022349	10.238726
O	21.459892	-22.827517	12.208641
O	19.403502	-22.080943	12.752548
H	17.560305	-21.424680	8.301433
H	18.448900	-21.158548	10.608924
H	21.499642	-24.674594	11.210355
C	18.538587	-24.384642	5.824801
H	17.989237	-24.246652	4.893334
H	18.270051	-25.350356	6.267704
H	19.615132	-24.360254	5.621625

Table S18. Product Structure for X= OMe (-1035.01192224 E_h)

atom	x	y	z
C	20.003338	-29.102597	10.986863
C	18.989988	-28.149943	11.173414
C	19.148156	-26.838789	10.714075
C	20.343537	-26.485997	10.067228
C	21.367573	-27.464310	9.867011
C	21.197606	-28.765299	10.326995
H	19.860909	-30.115711	11.350523
H	18.071578	-28.434676	11.677543
H	18.353582	-26.111902	10.853885
H	21.967564	-29.516940	10.178179
C	22.462286	-26.818213	9.133200
C	22.076949	-25.461450	8.888866
C	22.948892	-24.591157	8.212125
C	24.182424	-25.079656	7.771537
C	24.551654	-26.413299	8.006614
C	23.693269	-27.290130	8.692782
H	22.674073	-23.555947	8.034772
H	24.863942	-24.419164	7.244265
H	25.515022	-26.772597	7.657585
H	23.996391	-28.317619	8.872477
C	19.976970	-24.000074	9.364348
C	19.698198	-23.534024	8.064884
C	18.872778	-22.422462	7.858000
C	18.305556	-21.760221	8.961152
C	18.586103	-22.204585	10.241174
C	19.431097	-23.307641	10.475418
H	20.103907	-24.082757	7.224866
O	18.554789	-21.923068	6.638221
C	19.735145	-23.591423	11.908861
C	20.773932	-25.235997	9.474605
O	20.906048	-24.193176	12.223372
O	18.998513	-23.257360	12.823872
H	17.663073	-20.902647	8.792638
H	18.168995	-21.684226	11.095984
H	21.423442	-24.411405	11.428872
C	19.097619	-22.545152	5.465041
H	18.715737	-21.966174	4.625044
H	18.759532	-23.582973	5.380475
H	20.191505	-22.506527	5.472324

Table S19. Reactant Structure for X= NH_2 (-976.01488810 E_h)

atom	x	y	z
C	19.859654	-29.141085	10.418643
C	19.057588	-28.193444	11.071251
C	19.396146	-26.833279	11.045161
C	20.540359	-26.433039	10.358488
C	21.345436	-27.386398	9.697699
C	21.009952	-28.744831	9.727801
H	19.584425	-30.191518	10.448831
H	18.166366	-28.516619	11.601694
H	18.769373	-26.103775	11.551432
H	21.626794	-29.483808	9.223626
C	22.468125	-26.684459	9.058750
C	22.344328	-25.304263	9.329119
C	23.282861	-24.402840	8.831466
C	24.350089	-24.885763	8.061334
C	24.475369	-26.257387	7.796141
C	23.535952	-27.167044	8.293388
H	23.189903	-23.338852	9.032003
H	25.086783	-24.191924	7.666417
H	25.308468	-26.616092	7.198343
H	23.638338	-28.228364	8.084009
C	20.161792	-23.975641	9.699986
C	19.633124	-24.145533	8.412052
C	18.706677	-23.250171	7.859383
C	18.288786	-22.159738	8.645497
C	18.790945	-22.003184	9.932017
C	19.740482	-22.881593	10.489491
H	19.951128	-25.001593	7.820562
N	18.255134	-23.403761	6.543875
C	20.240183	-22.571195	11.902223
C	21.134117	-25.037220	10.213352
O	21.442433	-22.860235	12.189910
O	19.413123	-22.015374	12.683998
H	17.571648	-21.446198	8.246831
H	18.448361	-21.172690	10.540619
H	21.492235	-24.687108	11.188975
H	18.309169	-24.345777	6.176589
H	17.357489	-22.980164	6.344005

Table S20. Product Structure for X= NH_2 (-975.85044544 E_h)

atom	x	y	z
C	20.012183	-29.111014	10.986300
C	18.997528	-28.158554	11.167810
C	19.154469	-26.849432	10.702429
C	20.349331	-26.498860	10.053366
C	21.375487	-27.476460	9.859716
C	21.206753	-28.775434	10.326108
H	19.870707	-30.122518	11.354845
H	18.079428	-28.442001	11.673305
H	18.360899	-26.120968	10.839886
H	21.977943	-29.526780	10.182075
C	22.470009	-26.831747	9.124323
C	22.082016	-25.476807	8.873327
C	22.951203	-24.608570	8.190611
C	24.185920	-25.096541	7.752791
C	24.558518	-26.427980	7.995692
C	23.702083	-27.303244	8.686360
H	22.671821	-23.575752	8.006388
H	24.865775	-24.437746	7.221196
H	25.522752	-26.786913	7.648610
H	24.007305	-28.329298	8.870848
C	19.973164	-24.019040	9.328368
C	19.674774	-23.591068	8.028930
C	18.838048	-22.484947	7.777352
C	18.284637	-21.800241	8.881200
C	18.586010	-22.207249	10.169167
C	19.437865	-23.297983	10.433800
H	20.067988	-24.155111	7.188676
N	18.522845	-22.122197	6.488778
C	19.765835	-23.526405	11.865288
C	20.778125	-25.250244	9.456022
O	20.903050	-24.192933	12.183863
O	19.083236	-23.099473	12.786881
H	17.632303	-20.947639	8.717458
H	18.179431	-21.659978	11.012478
H	21.380992	-24.486471	11.388293
H	19.113215	-22.454423	5.739257
H	18.129614	-21.204313	6.335475

References

1. Becke, A. D., Density-Functional Thermochemistry. Iii. The Role of Exact Exchange. *J. Chem. Phys.* **1993,** *98*, 5648-5652.
2. Lee, C.; Yang, W.; Parr, R. G., Development of the Colle-Salvetti Correlation-Energy Formula into a Functional of the Electron Density. *Phys. Rev. B* **1988,** *37*, 785-789.
3. Hehre, W. J.; Ditchfield, R.; Pople, J. A., Self-Consistent Molecular Orbital Methods. Xii. Further Extensions of Gaussian—Type Basis Sets for Use in Molecular Orbital Studies of Organic Molecules. *J. Chem. Phys.* **1972,** *56*, 2257-2261.
4. Clark, T.; Chandrasekhar, J.; Spitznagel, G. W.; Schleyer, P. V. R., Efficient Diffuse Function-Augmented Basis Sets for Anion Calculations. Iii. The 3-21+G Basis Set for First-Row Elements, Li–F. *J. Comput. Chem.* **1983,** *4*, 294-301.
5. Hariharan, P. C.; Pople, J. A., The Influence of Polarization Functions on Molecular Orbital Hydrogenation Energies. *Theor. Chim. Acta* **1973,** *28*, 213-222.
6. Frisch, M. J.; Trucks, G. W.; Schlegel, H. B.; Scuseria, G. E.; Robb, M. A.; Cheeseman, J. R.; Scalmani, G.; Barone, V.; Petersson, G. A.; Nakatsuji, H.; Li, X.; Caricato, M.; Marenich, A.; Bloino, J.; Janesko, B. G.; Gomperts, R.; Mennucci, B.; Hratchian, H. P.; Ortiz, J. V.; Izmaylov, A. F.; Sonnenberg, J. L.; Williams-Young, D.; Ding, F.; Lipparini, F.; Egidi, F.; Goings, J.; Peng, B.; Petrone, A.; Henderson, T.; Ranasinghe, D.; Zakrzewski, V. G.; Gao, J.; Rega, N.; Zheng, G.; Liang, W.; Hada, M.; Ehara, M.; Toyota, K.; Fukuda, R.; Hasegawa, J.; Ishida, M.; Nakajima, T.; Honda, Y.; Kitao, O.; Nakai, H.; Vreven, T.; Throssell, K.; Jr, J. A. M.; Peralta, J. E.; Ogliaro, F.; Bearpark, M.; Heyd, J. J.; Brothers, E.; Kudin, K. N.; Staroverov, V. N.; Keith, T.; Kobayashi, R.; Normand, J.; Raghavachari, K.; Rendell, A.; Burant, J. C.; Iyengar, S. S.; Tomasi, J.; Cossi, M.; Millam, J. M.; Klene, M.; Adamo, C.; Cammi, R.; Ochterski, J. W.; Martin, R. L.; Morokuma, K.; Farkas, O.; Foresman, J. B.; Fox, D. J., Gaussian 09 Revision D.01. **2013**.
7. Miertuš, S.; Scrocco, E.; Tomasi, J., Electrostatic Interaction of a Solute with a Continuum. A Direct Utilizaion of Ab Initio Molecular Potentials for the Prevision of Solvent Effects. *Chem. Phys.* **1981,** *55*, 117-129.
8. Hansch, C.; Leo, A.; Taft, R. W., A Survey of Hammett Substituent Constants and Resonance and Field Parameters. *Chem. Rev.* **1991,** *91*, 165-195.
9. Darcy, J. W.; Kolmar, S. S.; Mayer, J. M., Transition State Asymmetry in C-H Bond Cleavage by Proton-Coupled Electron Transfer. *J. Am. Chem. Soc.* **2019,** *141*, 10777-10787.